Microbial origin of early animal trace fossils?

G. Mariotti[1,2], S. B. Pruss[3], X. Ai[4], J.T. Perron[2], T. Bosak[2]

1. Louisiana State University, Department of Oceanography and Coastal Sciences, Baton Rouge, LA, USA.

2. Massachusetts Institute of Technology, Department of Earth, Atmospheric and Planetary Sciences, Cambridge, MA, USA.

3. Smith College, Department of Geosciences, Northampton, MA, USA.

4. University of Science and Technology of China, School of Earth and Space Sciences**,** Hefei, Anhui, China.

Supplemental Material

1. Additional images of trace fossils

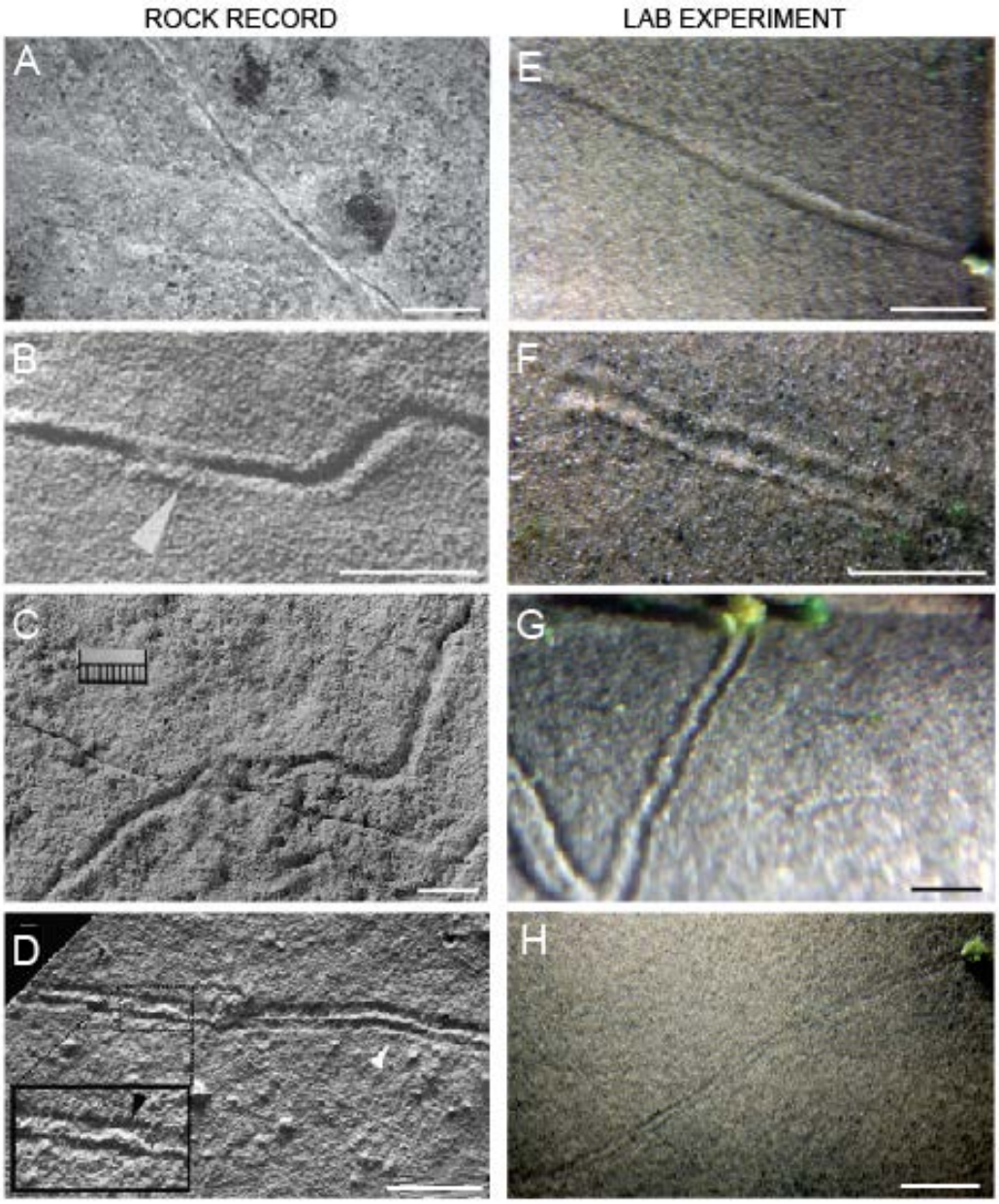

Figure S1. Comparison between trace fossils (A,B,C,D) and experimentally created trails (E,F,G,H). Trace fossil images from (A) Mistaken Point Formation, Newfoundland, 565 Ma (Liu et al. 2010); (B) Rawnsley Quartzite, Ediacara Range (Jenkins 1995); (C) Vindhyan Supergroup, Central India, > 1Ba (Seilacher et al. 1998); (D) Tacuarí Formation in east-central Uruguay, >585 Ma (Pecoits et al. 2012). All scale bars are 1 cm long.

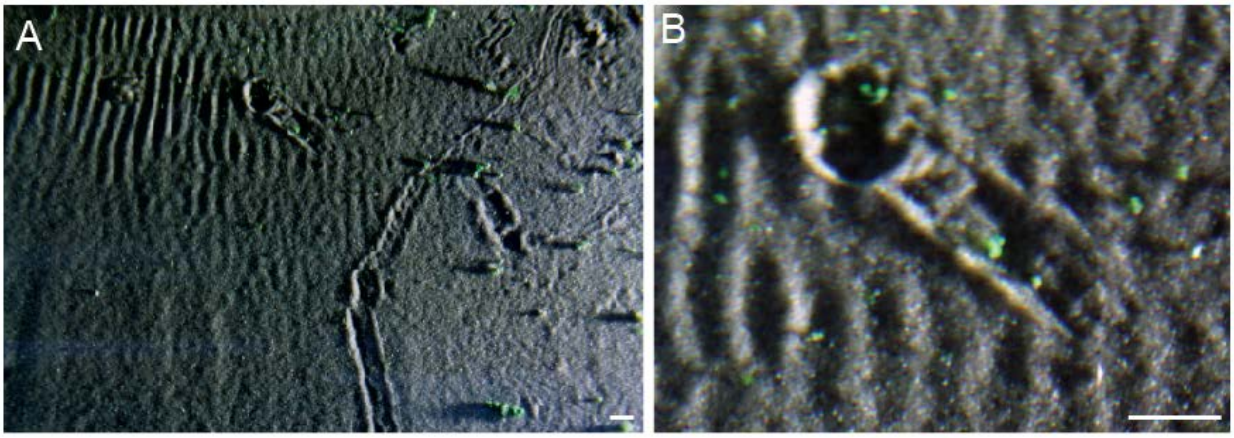

Figure S2. Trails and wrinkle structures formed on the same bed. (A) Lower magnification, photograph. (B) Detail of a trail ending in a large circular pit, created by an aggregate that oscillated around the same spot. All scale bars are 1 cm long.

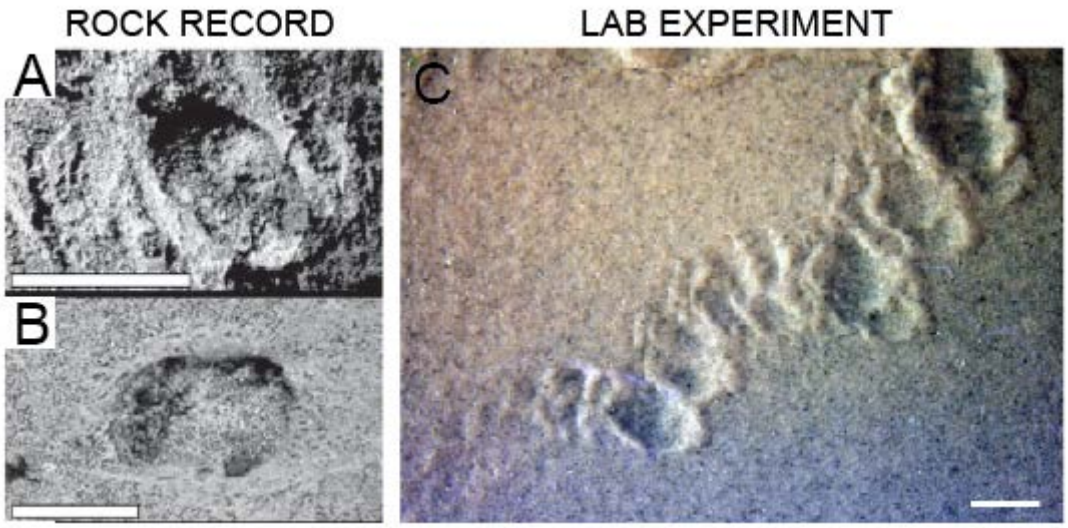

Figure S3. Scour features in the rock record (A,B) and generated by 10-20 mm large aggregates in the lab experiments (C). See Videos 14-17. Trace fossil images from (A,B) Mistaken Point Formation, Newfoundland, 565 Ma (Liu et al. 2010). All scale bars are 1 cm long.

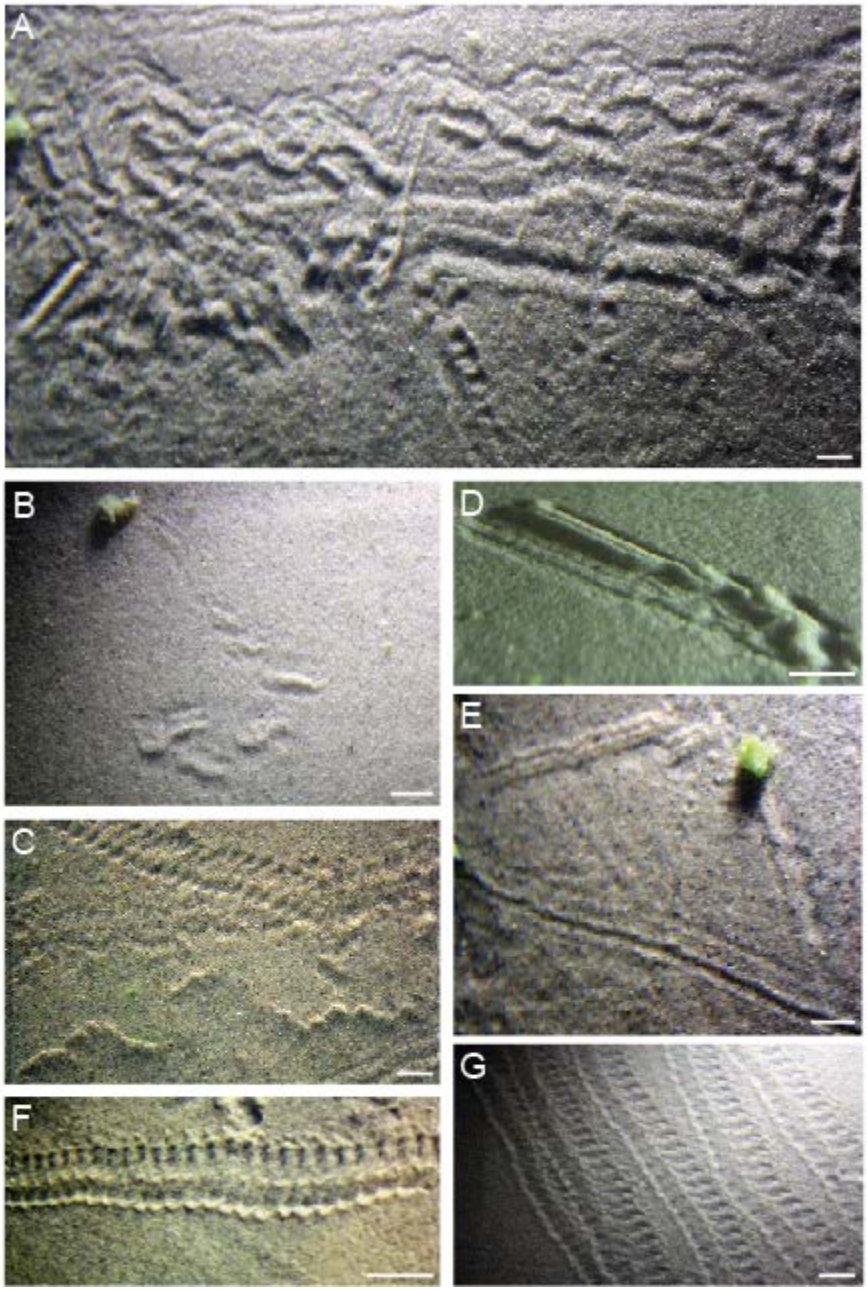

Figure S4. Variety of traces produced by microbial aggregates. (A) Intricate network of traces, overlapping with some pitted wrinkle structures. (B,C) Series of short, 1-2 cm long, isolated and randomly oriented ridged trails. (D,E) Ridged trail with small incision on the crest. Compare the ridged and grooved trails in (E). (F) Pitted tracks with oblate rims. (G) Tracks with asymmetric but regular pits. All scale bars are 1 cm long.

2. Characterization of the microbial aggregates

Microbial aggregates with a diameter of 5-25 mm were created by disaggregating a >1 yr old cyanobacterial mat, dominated by filamentous cyanobacteria, that had been grown in artificial seawater in another tank (Mariotti et al., 2014). Aggregates had a variable amount of sand attached to them, and some of the larger aggregates (>20 mm) were underlain by a thin layer of sand.

Total carbohydrate content of the microbial aggregates was measured with a modified phenol-sulfuric acid assay (Underwood et al., 1995). Given the aggregates trapped variable amounts of trapped sand grains, and that these grains were the heaviest parts of the fragments of microbial mats, the amount of carbohydrates cannot be accurately described by quantifying the glucose equivalents per gram dry weight. Instead, we measured the volume of the aggregates and converted it into equivalent grams of dry weight sediment using the standard density of dry sediment (1600 kg/m^3). The total amount of carbohydrates was then quantified as μg glucose / g equivalent weight of dry sediment. Two ml of distilled H_2O followed by 1 ml of 5% aqueous phenol (wt/vol) and 5 ml of concentrated sulfuric acid were added to each aggregate. The samples were left to react for 20 minutes and were then centrifuged at 3000 rpm for 10 minutes. The absorbance was measured against a reagent blank at 485 nm and the sample readings were compared to the standard curve for the absorption of glucose solution treated in the same manner. The carbohydrate content in six samples was measured, yielding an average value of 713 μg/g of total carbohydrate and a standard deviation of 155 μg/g. Similar values are found in biofilms from sandy and muddy tidal flats (Underwood and Smith 1998), indicating that experimental microbial aggregates were comparable to natural photosynthetic mats.

3. Net transport

Net transport occurred at different angles with respect to the direction of the wave oscillation, indicating that residual flows in the tank did not cause this net transport. Instead, we hypothesize that the

net transport was due to asymmetries in the shapes of the aggregates. In a manner similar to the sail of a boat, the aggregate experiences a force directed at an angle with respect to the direction of the oscillatory motion (Wetzel 1999) (Fig. 2). To test this hypothesis, we produced a track with a single aggregate and then rotated the aggregate by 180 degrees using tweezers, without interfering with the flow (Video 12). The aggregate reversed its direction and produced a trail that ran in the opposite direction from the initial trail (Video 12).

Larger microbial aggregates can entrain and trap sand grains, which provide ballast and change the aggregates' mass distributions during the few minutes necessary to form trails. This effect contributes to sudden changes in aggregate motion and the resulting trail morphology.

4. Experiments with a progressive wave

To test whether the standing wave used in the experiments was necessary to create the observed motion of the aggregates, we repeated some experiments in a 60 cm wide, 50 cm deep and 7 m long tank in which a progressive wave was generated by a mechanical paddle (Nienhuis et al. 2014). The bottom of the tank was covered with a layer of silica sand with a median diameter of 0.18 mm and filled with fresh water. A wave with a height of 15 cm and a period of 1.5 s was generated in a water depth of 16 cm. The sand bed was flattened and five 10-20 cm wide aggregates used in the previous experiments were dropped on the bed surface. The aggregates oscillated, moved and created grooved and pitted trails similar to those obtained with the standing wave (Fig. S5). As predicted, the nature of the wave motion is not a determinant factor for the formation of trails by moving microbial aggregates.

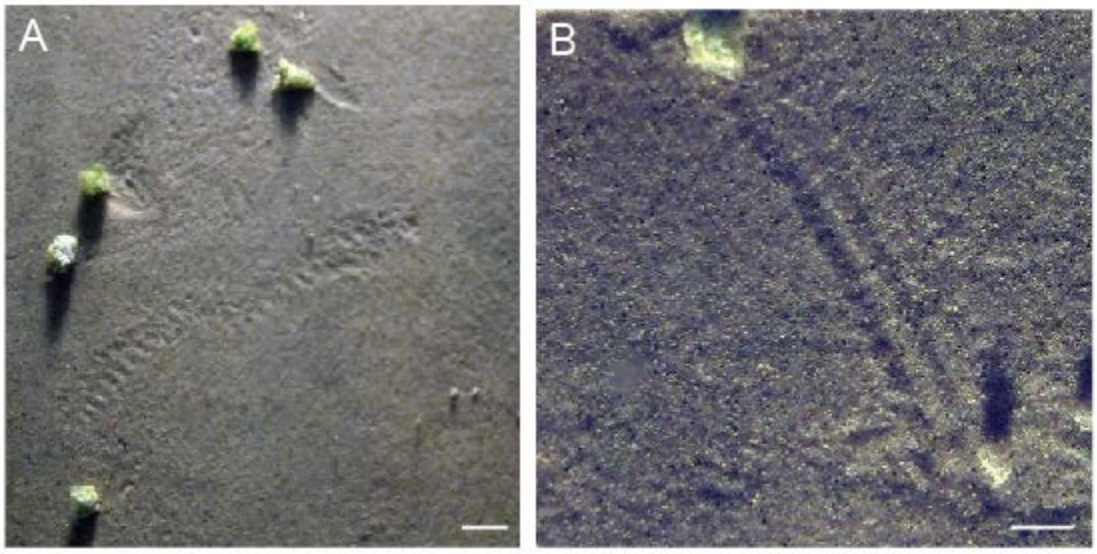

Figure S5. Pitted (A) and grooved (B) trails formed in a 7 m long tank with a progressive wave, using the same microbial aggregates as in the experiments with a standing wave. All scale bars are 1 cm long.

References

Jenkins, R.J.F., 1995, The problems and potential of using animal fossils and trace fossils in terminal Proterozoic biostratigraphy: Precambrian Research, v. 73, no. 1–4, p. 51–69, doi: 10.1016/0301-9268(94)00071-X.

Liu, A.G., Mcllroy, D., and Brasier, M.D., 2010, First evidence for locomotion in the Ediacara biota from the 565 Ma Mistaken Point Formation, Newfoundland: Geology, v. 38, no. 2, p. 123–126, doi: 10.1130/G30368.1.

Mariotti, G., Perron, J.T., and Bosak, T., 2014, Feedbacks between flow, sediment motion and microbial growth on sand bars initiate and shape elongated stromatolite mounds: Earth and Planetary Science Letters, v. 397, p. 93–100, doi: 10.1016/j.epsl.2014.04.036.

Nienhuis, J.H., Perron, J.T., Kao, J.C.T., and Myrow, P.M., 2014, Wavelength selection and symmetry breaking in orbital wave ripples: Journal of Geophysical Research: Earth Surface, v. 119, no. 10, p. 2239–2257, doi: 10.1002/2014JF003158.

Pecoits, E., Konhauser, K.O., Aubet, N.R., Heaman, L.M., Veroslavsky, G., Stern, R.A., and Gingras, M.K., 2012, Bilaterian burrows and grazing behavior at >585 Million years ago: Science, v. 336, no. 6089, p. 1693–1696, doi: 10.1126/science.1216295.

Seilacher, A., Bose, P.K., and Pfluger, F., 1998, Triploblastic animals more than 1 billion years ago: trace fossil evidence from India: Science, v. 282, no. 5386, p. 80–83.

Underwood, G.J.C., Paterson, D.M., and Parkes, R.J., 1995, The measurement of microbial carbohydrate exopolymers from intertidal sediments: Limnology and Oceanography, v. 40, no. 7, p. 1243–1253, doi: 10.4319/lo.1995.40.7.1243.

Underwood, G.J.C., and Smith, D.J., 1998, Predicting epipelic diatom exopolymer concentrations in intertidal sediments from sediment chlorophyll a: Microbial Ecology, v. 35, no. 2, p. 116–125, doi: 10.1007/s002489900066.

Wetzel, A., 1999, Tilting marks: a wave-produced tool mark resembling a trace fossil: Palaeogeography, Palaeoclimatology, Palaeoecology, v. 145, no. 1–3, p. 251–254, doi: 10.1016/S0031-0182(98)00096-0.

List of videos

Video1. Wide single-groove trail. Speed 30X.

Video 2. Thin single groove with levees. Speed 30X.

Video 3. Thin single groove with levees. Speed 60X.

Video 4. Linear pitted trail parallel to the wave direction. Speed 30X.

Video 5. Complex pitted trail, geometry varies along the trail. Speed 30X.

Video 6. Seven different grooved trails that intersect. Speed 150X.

Video 7. Grooved trail that stops and restarts a few centimeters apart. Speed 30X.

Video 8. Grooved trail that curves. Speed 30X.

Video 9. Grooved trail that zigzags. Speed 150X.

Video 10. Scour hole formed by a large fragments trapped in the same spot. Speed 150X.

Video 11. Linear trails formed on a bed where ~ 1 mm wide microbial aggregates had previously formed ridged wrinkle structures. The wave conditions were the same during the formation of wrinkle structures and linear trails. Speed 30X.

Video 12. Fragment that moves perpendicular to the wave direction. The same fragment is manually rotated by 180 degrees after 2 and after 10 seconds from the beginning of the video. After each rotation the net transport direction reverses. This video shows that the aggregate geometry rather than the bed slope or residual flow in the tank dictates the direction of net transport. Speed 30X.